

Absolute negative mobility induced by potential phase modulation

Bruno S. Dandogbessi

Theoretical Physics Department, African University of Science and Technology, Km 10 Airport Road, Galadimawa, Abuja, Nigeria

Anatole Kenfack*

Physikalische und Theoretische Chemie, Institut für Chemie und Biochemie, Freie Universität Berlin, Takustraße 3, DE-14195 Berlin, Germany

(Received 24 September 2015; published 2 December 2015)

We investigate the transport properties of a particle subjected to a deterministic inertial rocking system, under a constant bias, for which the phase of the symmetric spatial potential used is time modulated. We show that this modulated phase, assisted by a periodic driving force, can lead to the occurrence of the so-called absolute negative mobility (ANM), the phenomenon in which the particle surprisingly moves against the bias. Furthermore, we discover that ANM predominantly originates from chaotic-periodic transitions. While a detailed mechanism of ANM remains unclear, we show that one can manipulate the control parameters, i.e., the amplitude and the frequency of the phase, in order to enforce the motion of the particle in a given direction. Finally, for this experimentally realizable system, we devise a two-parameter current plot which may be a good guide for controlling ANM.

DOI: [10.1103/PhysRevE.92.062903](https://doi.org/10.1103/PhysRevE.92.062903)

PACS number(s): 05.45.-a, 05.90.+m, 05.60.Cd, 82.40.Bj

I. INTRODUCTION

A common expectation is that particle transport in a system follows the direction of the applied bias. However, counterexamples are found in systems where such a particle can, instead, travel in a direction opposite to the applied bias. One thus speaks of absolute negative mobility (ANM), a phenomenon which has attracted the attention of researchers in the directed transport community during the last decade (see Ref. [1] and references therein). ANM was originally perceived as being solely due to quantum mechanical effects [2] which may not survive in the classical limit. However, further investigations have revealed the occurrence of this phenomenon in classical dynamical systems. The first class of classical systems exhibiting ANM consists of a variety of models of interacting Brownian particles whereby the collective effects are responsible for the onset of ANM [3–10]. But at the time those models were first considered, it was commonly presumed that a single particle cannot manifest ANM [1]. Shortly afterwards, ANM was demonstrated in a system where a single Brownian particle was allowed to move along meandering paths in a conveniently tailored channel with inner walls [11–14]. Also, an affordable working concept for a classical ANM device was proposed by embedding spatial asymmetry into the shape of the transported particles [15], much like the case of a particle exposed to a two-dimensional square lattice of Ref. [16].

In the systems mentioned above, noise actually played a constructive role, much like in systems exhibiting stochastic resonance [17]. This framework of noise-induced ANM with a single particle turned out to be a very active field of research, which rapidly led to more and more interesting outcomes [18–21], including ANM in Josephson junctions that constitute realistic examples [22,23]. While ANM is

enhanced for an appropriate amount of noise in a purely noise-induced case [18], this phenomenon may be weakened as the temperature increases in the presence of chaos in an underdamped system where the particle mass is significant [19,20]. In an overdamped regime, a spatially symmetric and periodic system is likely to manifest ANM in the presence of the time delay feedback [24].

Recently, the role usually played by noise in stochastic resonance has been conveniently replaced by a time periodic signal, thereby leading to a new phenomenon called vibrational resonance [25,26]. In this framework, ANM was observed in a system termed a “vibrational motor” following the terminology of the vibrational resonance [27]. Here, ANM originated from the combination of two periodic driving signals which, together, are asymmetric under time reversal. Even more surprising is that ANM was observed in a deterministic system evolving in a periodic and symmetric potential subjected to external unbiased periodic driving and nonuniform space-dependent damping [28].

Motivated by the manifestation of ANM in a driven single-particle system in the absence of noise, we propose a model for which the phase of the symmetric standing potential is modulated in time. Interestingly, such a potential can be designed experimentally and its phase modulation has been found to cause the Rabi oscillations observed in an optical potential system [29]. The question that we ask now is whether such a system can exhibit ANM. If so, what then could be the origin and the mechanism of this unexpected phenomenon? To the best of our knowledge, these questions have not yet been addressed in the model of the present study.

This paper is organized as follows. In Sec. II, we introduce our model system and provide ingredients for particle-current computations. We show in Sec. III that the occurrence of ANM is due to the potential phase modulation. Then the origin as well as the mechanism of ANM are discussed. Finally, in Sec. IV we show that ANM can be systematically controlled as a function of phase parameters and we summarize the main results of this paper in Sec. V.

*kenfack@zedat.fu-berlin.de

II. MODEL DESCRIPTION

Consider a single particle in a spatially phase-modulated symmetric potential subjected to external fields. The dynamics of this system is deterministic and is governed by the dimensionless equation of motion of the form

$$\frac{d^2x}{dt^2} + \gamma \frac{dx}{dt} = -\frac{\partial V(x,t)}{\partial x} + F(t) + f, \quad (1)$$

where $x = x(t)$ denotes the spatial coordinate of the particle at time t . Here, γ is a damping parameter, f a constant load, $F(t) = q \cos(\Omega t)$ a periodic driving force of amplitude q and frequency Ω , and $V(x,t)$ the spatial time-dependent potential given by

$$V(x,t) = -V_0 \sin[x - \phi(t)], \quad (2)$$

where $\phi(t) = \lambda \cos(\beta t)$ stands for the time-dependent periodic phase of amplitude λ and frequency β , and V_0 the normalized amplitude. Thanks to Raizen *et al.* [29], such a potential can be prepared by counterpropagating two laser beams in order to build up a one-dimensional optical lattice potential for which the phase can be conveniently time modulated. The associated experimental setup could then correspond to a very weakly damped alkali atom, a cesium atom for instance, trapped in this optical lattice potential $V(x,t)$ and subject to external driving forces. Note that the applied load f implies an added potential $-xf$ to the system. When $\lambda = 0$, one recovers the standing sinusoidal potential $V_0 \sin(x)$, while the nonzero phase induces a time-dependent shift along the spatial coordinate of this potential. In particular, for small λ , one can shed light on the effect of this phase modulation by expanding the potential to first order in λ as $V(x,t) = -V_0 \sin(x) + V_0 \lambda \cos(x) \cos(\beta t)$. Clearly, the second term of the expansion adds a harmonic driving force that is very likely to induce important changes in the system. This was responsible for the Rabi oscillations observed in Ref. [29]. Observe that $\int_0^{2\pi/\Omega} F(t) dt = 0$ and $\int_0^{2\pi} V(x,t) dx = 0$, so that the resulting average of $F(t)$ and $V(x,t)$ over space and time on the particle is nil.

The system of Eq. (1), without the modulated phase $\phi(t)$, has been an active field where ANM has been detected, but in the presence either of noise and/or periodic driving forces or in the presence of two driving forces (vibrational resonance) as elucidated in Sec. I. Here, this counterintuitive ANM effect is explored by modulating the phase of the spatial potential, in the presence of one driving force and in the absence of noise.

The behavior of this system is examined by calculating the current. Because not only transient chaos may be present, but also different types of attractors may coexist, the computation of this current must account for well defined statistical considerations. On that basis, Mateos [30] intuitively defined the current J as the time average of the average velocity over an ensemble of initial conditions. Specifically an average can be performed at a given observation time t_j for several trajectories $x_i(t_j)$ calculated with different initial conditions $x_i(0)$ and $\dot{x}_i(0)$. This yields the average velocity as

$$v_j = \frac{1}{N} \sum_{i=1}^N \dot{x}_i(t_j), \quad (3)$$

where the overdot denotes the time derivative and N the number of initial conditions used. The current is finally obtained by time averaging the velocity above over the total number of observations M :

$$J = \frac{1}{M} \sum_{j=1}^M v_j. \quad (4)$$

In practice, the computation of this current may be very time consuming; especially in the chaotic situation where a very large number of trajectories is needed and a very long observation time is required. To circumvent this difficulty, Kenfack *et al.* realized that the convergence can be accelerated just by ruling out the transients [31]. This results in modifying the current formula in Eq. (4) to

$$J = \frac{1}{M - M_c} \sum_{j=M_c+1}^M v_j, \quad (5)$$

where M_c is some empirical cutoff number accounting for the transients. Remarkably this task becomes simplified, relying on a single trajectory calculation, if the system is exempt from chaos.

In our numerical experiments, performed using the Runge-Kutta algorithm to solve Eq. (1), we could achieve converged currents using an ensemble of $N = 1000$ initial conditions randomly distributed about the origin of the coordinate axis, with the associated velocities fixed at zero. With a time step $\Delta t = 0.09$, the transient-discard time at $M_c = 1000$ was sufficient and the total observation time was set to $M = 10^6$. Throughout the paper, the potential amplitude $V_0 = 1$ and the damping coefficient $\gamma = 0.108$ are kept fixed, while other parameters may be purposely tuned. In the next section, we will explore the dynamics of our system, focusing on the behavior of the particle current, a plausible indicator of the absolute negative mobility.

III. ABSOLUTE NEGATIVE MOBILITY IN THE PHASE-MODULATED DRIVEN TILTED POTENTIAL

To appreciate the influence of the phase modulation on our particle current J , it is instructive to first explore the dynamics at zero phase modulation. We solve Eq. (1) numerically as discussed in the previous section.

A. Zero-phase dynamics

In the absence of the phase, i.e., with $\lambda = 0$, the current has been computed as a function of the constant load f and is depicted in Fig. 1. When the driving force $F(t)$ is switched off ($q = 0.0$), no current is generated for any value of f less than the critical force $f_c = V_0$; the particle, actually trapped inside the potential well, leads to zero particle transport [see dashed red line in Fig. 1(a)]. But once f is larger than the potential barrier V_0 , which has been set to unity, the particle will typically follow the direction of the constant load with the current J generally proportional to f . On the other hand, when the system is driven out of equilibrium with the help of the driving force $F(t)$ (i.e., $q \neq 0$), the dynamics is expected to be richer as chaos may come into play. Figure 1(a), solid blue line, shows the nonzero current as a function of the constant load

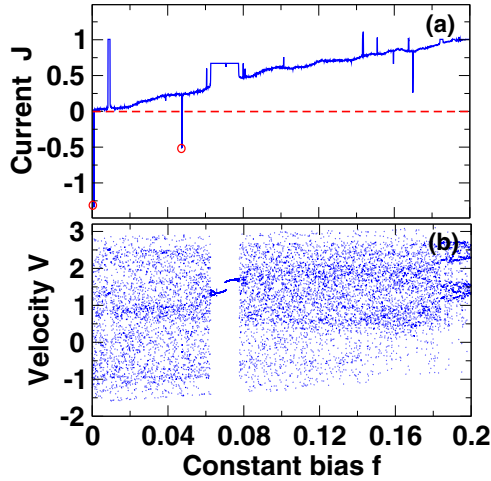


FIG. 1. (Color online) (a) The current as a function of the bias f , with $\lambda = 0.0$, for $q = 0.0$ (dashed red line) where $J \equiv 0$ and for $q = 1.12$ (solid blue line). (b) The bifurcation diagram associated with (a) for $J \neq 0$. One sees a periodic window $f \in (0.0631, 0.0776)$ with a constant current and chaotic regions exhibiting jumps that can lead to ANM (red circle) at $f = 0.001$ and $f = 0.0478$.

$f < f_c$. The overall behavior shows an increasing current as f increases but with some sudden jumps. To obtain more insight into such current behavior, the associated bifurcation diagram has been computed; see Fig. 1(b). One can clearly distinguish two regimes: (i) the regime of regular motion for which the current is constant within the window $f \in (0.0631, 0.0776)$; and (ii) the regime of chaotic motion which is predominant here. It is precisely in the chaotic regime that these erratic jumps appear in the current. One such jump has a direct effect of enhancing the current and may in few isolated cases lead to absolute negative mobility; see red circles in Fig. 1(a). In ratchet systems, that is, in the absence of the bias ($f = 0$), such negative currents were found at the chaos-periodic transition, often leading to the so-called current reversal [30–32].

B. Influence of the phase modulation

Besides the periodic driving force $F(t)$, the modulation of the potential phase constitutes another important source intended to drive the system out of equilibrium. Indeed, when the time-dependent phase $\phi(t)$ is switched on, this standing potential is time-shifted back and forth along the position coordinate of the particle.

In the absence of the driving force $F(t)$, $q = 0$, and for $\beta = 0.67$, the current of the particle under the phase modulation is displayed in Fig. 2 as a function of the applied load f for $\lambda = 0.0$ (dashed red line) and for $\lambda = 2.0$ (solid blue line). The nonzero current here with $\lambda = 2$ is clear evidence that the phase is responsible of the particle motion since no current is revealed for $\lambda = 0$. In this case, one distinguishes a periodic regime where the current is constant and the chaotic ones where the behavior of the current is not predictable. In fact, in this chaotic regime, the current J monotonically increases from zero up to $J = 0.07$ and then remains on average around this value of the current with a few instances of jumps that induce significant changes. The

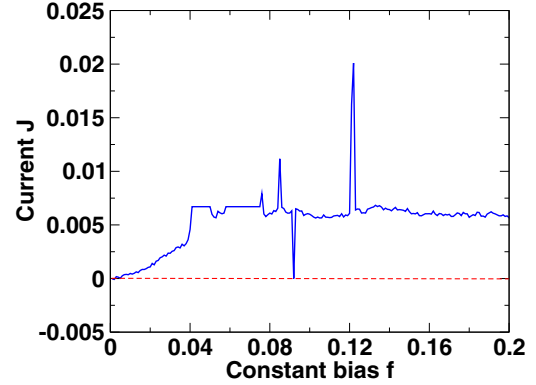


FIG. 2. (Color online) The current as a function of the bias f in the absence of periodic driving ($q = 0.0$). Here J is identically zero for $\lambda = 0.0$ (dashed red line). But, for $\lambda = 2.0$ (solid blue line), J is constant in the periodic regime, while in the chaotic regime J monotonically increases for $f \in (0.0, 0.035)$ and takes on erratic values for $f \in (0.035, 0.2)$.

corresponding bifurcation diagram (not shown) is actually consistent with the behavior observed here, much like in Fig. 1. Furthermore, it is worth mentioning that the dynamics becomes completely dominated by the constant load when $f > V_0$. In this case the current J increases linearly with f .

It is also worth mentioning that the general trend observed here for $\lambda = 2.0$ is similar to that obtained for a broad range of λ , including very small values.

Next, when the driving force is taken into account, $q \neq 0$, the current of the particle under the phase modulation, as in Fig. 2, is depicted in Fig. 3 as a function of the applied load f . Remarkably, a large window [$f \in (0.04, 0.125)$] of absolute negative mobility (ANM) emerges, with a strong current flowing in the direction opposite to the constant load. From the discussions above, we can infer that this counterintuitive

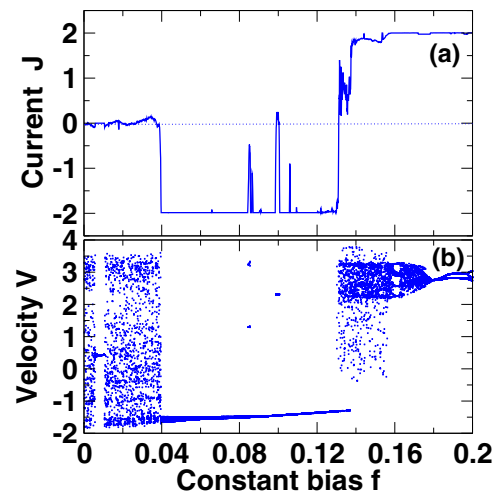


FIG. 3. (Color online) (a) The current as function of the bias f in the presence of the modulated phase $\phi(t) = \lambda \sin(\beta t)$ and the driving force $F(t) = q \cos(\Omega t)$ (solid blue line). Here $\lambda = 2.0$, $\beta = 0.67$, and $q = 1.12$. (b) The bifurcation diagram associated with (a) (dotted blue line). Remarkably, a large window $(0.04, 0.13)$ of absolute negative mobility occurs at chaotic-periodic transitions.

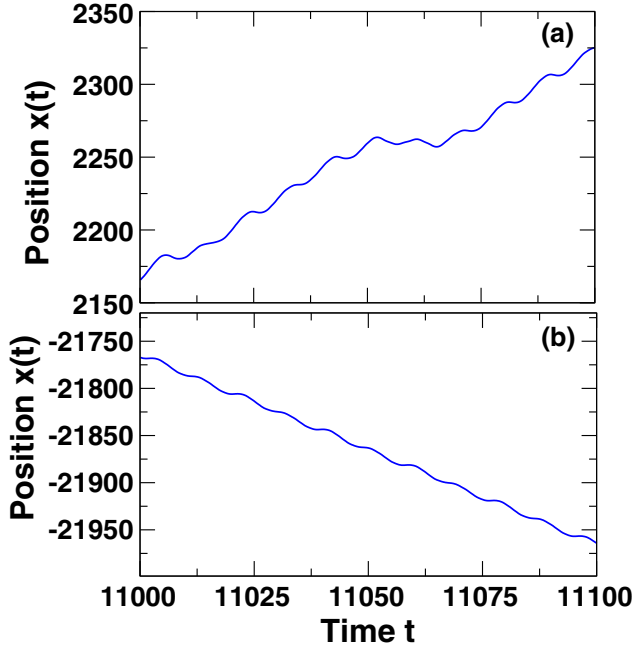


FIG. 4. (Color online) The trajectory of the particle for $f = 0.035$ (a), showing positive current, and for $f = 0.05$ (b), demonstrating the counterintuitive ANM [see Fig. 3(b)]. Here $q = 1.12$, $\beta = 0.67$, and $\lambda = 2.0$.

phenomenon is presumably due to the phase modulation assisted by the periodic driving force $F(t)$. In other terms, the periodic driving force $F(t)$ is a prerequisite for the phase modulation inducing ANM. Much like in the previous case, with $q = 0$, when the constant bias f is bigger than the critical value $f_c = V_0 + q$, the dynamics is dictated by f and the current transport J increases linearly with f .

C. Origin and mechanism of absolute negative mobility

In order to understand the origin of ANM here, we plot the bifurcation diagram in Fig. 3(b) (dotted blue line) corresponding to the current in Fig. 3(a) (solid blue line). One clearly sees, in this chaotic deterministic system, a pronounced correlation between both graphs. Jumps exhibited by the current happen precisely at tangent points where transitions between chaos and periodic orbits are produced. In particular, this behavior has led to ANM in the range $f \in (0.04, 0.125)$ in which a few jumps also appear to mimic again a similar type of transition with very few points in the bifurcation diagram. Outside this window, the current follows the bias both in periodic and chaotic regimes. Figure 4 displays the time series of particle position, highlighting the chaotic motion of the particle in the same direction with the constant load $f = 0.035$ (a) and, of special interest, the manifestation of ANM where a periodic orbit is being accelerated in the direction opposite to that of $f = 0.05$ (b).

Having explained the origin of ANM in this system, we can subsequently endeavor to follow the particle current in more detail in order to attempt to highlight the heuristic mechanism underlying this counterintuitive phenomenon. From our numerical results above, it turns out that ANM shows

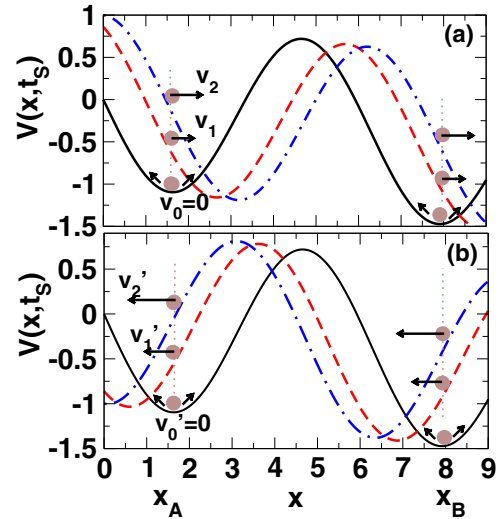


FIG. 5. (Color online) Potential $V(x, t_S)$ [Eq. (6)] highlighting the phase effect on a particle as a function of the particle position x and for two snapshot times t_S [(a) and (b)]. For $\lambda = 0$ (solid line), the particle (brown ball) sits at the bottom of the potential x_A or x_B with zero velocity ($v_0 = v'_0 = 0$), while for $\lambda = 2$ (dashed red line) and $\lambda = 3$ (dot-dashed blue line), the particle receives positive kicks v_1 and v_2 (a) and negative kicks v'_1 and v'_2 (b) likely to stimulate the occurrence of ANM.

up here as a result of the cooperation between the periodic driving force and the time-dependent phase of the potential. The driving force contributes to the periodic rocking of the potential, with equal probability of pulling the particle to the left and to the right since the potential is symmetric. This probability will of course be increased in the direction of an additional applied constant load with a few exceptions leading to ANM [see Fig. 1(a)] due to the presence of chaos in the system. However to uncover the role played by the phase on the particle, we first consider the case of zero phase (Fig. 2 with $\lambda = 0$) where only a constant load is applied and then the case where the time-dependent phase $\phi(t)$ is switched on (Fig. 2 with $\lambda = 2$). The latter is equivalent to exploring the particle in the following potential landscape:

$$V(x, t_S) = -V_0 \sin[x - \phi(t_S)] - xf, \quad (6)$$

where t_S is a given snapshot time. Figure 5 shows the particle in the potential of Eq. (6) [$V(x, t_S)$], as function of the position x , for different values of the phase λ and for two different configurations of the snapshot times t_S leading to positive velocities [Fig. 5(a)] and to negative velocities [Fig. 5(b)]. For $\lambda = 0$ (solid line), the particle experiences small oscillations in the bottom of the tilted potential, at positions x_A and x_B , with velocities which are on average zero ($V_0 = 0$ or $V'_0 = 0$). However, when the phase is switched on, i.e., $\lambda \neq 0$ (dashed line and dot-dashed line), this induces a shift that can drive the particle (brown ball) to the right in the direction of the constant load f or to the left (opposite to f), thereby contributing to cause ANM in this chaotic deterministic system. One can conclude that this phase and the periodic driving force cooperatively assist each other to move against the applied

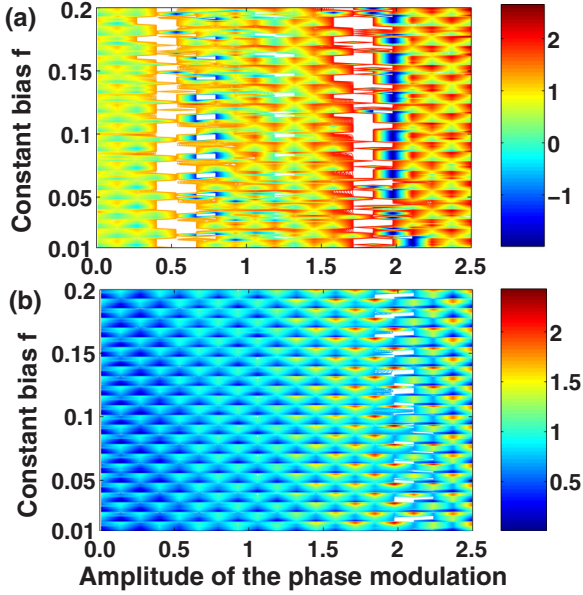


FIG. 6. (Color online) The (λ, f) prototypical current diagram plotted for $\beta = 0.67$ (a) and for $\beta = 4.5$ (b) with $q = 1.12$. In (a) islands of ANM emerge, while in (b) one observes instead a positive transport throughout with a regular periodic pattern with much lower constant currents, at $\lambda_c = 1.25$, as compared to much higher and irregular currents at $\lambda > \lambda_c$.

constant load, especially at the tangent points where transitions from chaos to periodicity happen.

IV. ABSOLUTE NEGATIVE MOBILITY CONTROL

In the previous section, ANM as well as its origin have been numerically demonstrated for isolated values of the modulated phase of the potential in the presence of the driving force. To allow for more systematic control of the occurrence of ANM, it would be enlightening to explore the current landscape for a much wider range of system parameters. Figure 6 displays the current as a function of both the amplitude of the modulated phase of the potential λ and the constant bias f , where $(\lambda, f) \in ((0.0, 2.5), (0.0, 0.2))$ with $q = 1.12$, for $\beta = 0.67$ (a) and for $\beta = 4.5$ (b). These two-parameter plots provide us with a global view of the current where regions of normal transport and regions of absolute negative mobility (ANM) transport are clearly uncovered for a constant load. In particular, in Fig. 6(b) the transport happens predominantly in the expected direction, that is, the direction of the constant load, with very few instances of ANM, which, when detected, is of the order of ($J = 10^{-4}$). Note also the emergence of a regular periodic pattern when $\lambda \leq \lambda_c = 1.25$ with much lower currents as compared to currents for $\lambda > \lambda_c$. On the other hand, one observes many islands of ANM in Fig. 6(a), which mostly show up at around $\lambda = 0.75$ and $\lambda = 2.0$. White regions correspond to almost zero current. It is important to notice that the dynamics explored in (β, f) space show a two-parameter diagram for which the probability of experiencing ANM is very small. Figure 7 depicts two plots extracted from such a (β, f) diagram (not shown) as a cut at $\lambda = 2.0$ for $f = 0.16$ [Fig. 7(a)], showing a completely positive current, and a cut for $f = 0.06$

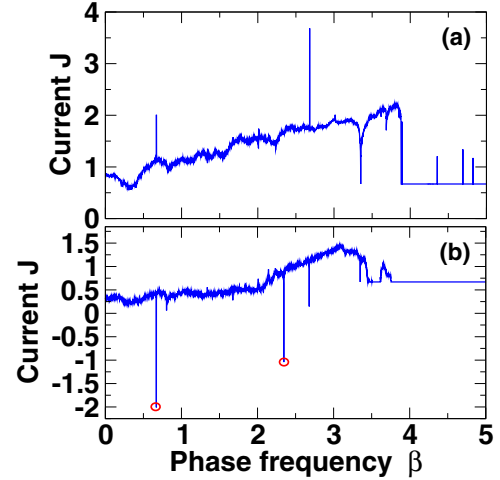


FIG. 7. (Color online) The current as a function of the phase frequency β for (a) $f = 0.16$ and (b) $f = 0.06$. Here $\lambda = 2.0$ and $q = 1.12$. In accordance with Fig. 3, the positive current is revealed in (a), while ANM (red circle) occurs in (b) at values $\beta = 0.67$ (used in Fig. 3) and $\beta = 2.34$.

[Fig. 7(b)] with two occurrences of ANM (red circle), in agreement with Fig. 3. Here, the value of the frequency of the phase $\beta = 0.67$ is well reproduced (Fig. 3) together with another one at $\beta = 2.34$. It is in such a landscape (Fig. 6) that ANM can be systematically controlled in this transport problem. In doing so, ANM can be avoided if not purposely desired. Finally it is crucial to point out that Fig. 6 is a prototypical plot which may constitute a useful guide for people conducting particle transport experiments in such a model [29].

V. CONCLUSION

To sum up, we have addressed the single-particle transport properties in an inertial periodically driven spatial symmetric phase-modulated potential and under the influence of a constant bias. With the amplitude λ and the frequency β of this time modulated phase as controlled parameters, we unveiled the striking phenomenon of absolute negative mobility (ANM) in which the particle counterintuitively moves against the constant bias. Having established that this is a cooperative effect between the phase modulation and the periodic driven force, we analyzed the relationship between the current and the bifurcation diagram. It turned out that this surprising phenomenon can be associated with the bifurcation from chaotic to periodic orbits, where the current exhibits remarkable jumps that can lead to a situation where the current reverses its direction (ANM) from the expected one. Although a proper mechanism is still not completely detailed, we were able to show that we can make use of the control parameters to increase the probability of the particle to move in a desired direction. To allow for a more systematic and global control of ANM, we constructed a two-parameter (λ, f) prototypical current diagram. We expect these results to stimulate people working in this field to conduct some experiments.

ACKNOWLEDGMENTS

We thank O. Akin-Ojo for useful discussions and for carefully reading the manuscript. A deep appreciation goes to C. Mulhern for his constructive remarks and comments. This work was supported by the African University of Science and Technology-Abuja Nigeria (AUST) and the Nelson Mandela

Institution (NMI). We also acknowledge the Center for High Performance Computing (CHPC) in South Africa and the Abdus Salam International Centre for Theoretical Physics (ICTP) in Trieste, Italy for computational resources. This work was supported by the World Bank African Centers of Excellence program of the African University of Science and Technology Abuja-Nigeria.

-
- [1] R. Eichhorn, P. Reimann, B. Cleuren, and C. Van den Broeck, *Chaos* **15**, 026113 (2005).
- [2] B. J. Keay, S. Zeuner, S. J. Allen, K. D. Maranowski, A. C. Gossard, U. Bhattacharya, and M. J. W. Rodwell, *Phys. Rev. Lett.* **75**, 4102 (1995).
- [3] P. Reimann, R. Kawai, C. Van den Broeck, and P. Hänggi, *Europhys. Lett.* **45**, 545 (1999).
- [4] P. Reimann, C. Van den Broeck, and R. Kawai, *Phys. Rev. E* **60**, 6402 (1999).
- [5] C. Van den Broeck, P. Reimann, R. Kawai, and P. Hänggi, in *Statistical Mechanics of Biocomplexity*, Proceedings of the XV Sitges Conference, Barcelona, June 1998, edited by D. Reguera, J. M. G. Vilar, and J. M. Rubi, Springer Lecture Notes in Physics Vol. 527 (Springer, Berlin, 1999), p. 93.
- [6] J. Buceta, J. M. Parrondo, C. Van den Broeck, and F. J. de la Rubia, *Phys. Rev. E* **61**, 6287 (2000).
- [7] C. Van den Broeck, I. Bena, P. Reimann, and J. Lehmann, *Ann. Phys. (N.Y.)* **9**, 713 (2000).
- [8] S. E. Mangioni, R. R. Deza, and H. S. Wio, *Phys. Rev. E* **63**, 041115 (2001).
- [9] B. Cleuren and C. Van den Broeck, *Europhys. Lett.* **54**, 1 (2001).
- [10] M. Januszewski and J. Łuczka, *Phys. Rev. E* **83**, 051117 (2011).
- [11] R. Eichhorn, P. Reimann, and P. Hänggi, *Phys. Rev. Lett.* **88**, 190601 (2002).
- [12] R. Eichhorn, P. Reimann, and P. Hänggi, *Phys. Rev. E* **66**, 066132 (2002).
- [13] R. Eichhorn, P. Reimann, and P. Hänggi, *Physica A* **325**, 101 (2003).
- [14] A. Ros, R. Eichhorn, J. Regtmeier, T. T. Duong, P. Reimann, and D. Anselmetti, *Nature (London)* **436**, 928 (2005).
- [15] P. Hänggi, F. Marchesoni, S. Savelev, and G. Schmid, *Phys. Rev. E* **82**, 041121 (2010).
- [16] D. Speer, R. Eichhorn, and P. Reimann, *Phys. Rev. Lett.* **102**, 124101 (2009).
- [17] L. Gammaitoni, P. Hänggi, P. Jung, and F. Marchesoni, *Rev. Mod. Phys.* **70**, 223 (1998); T. Wellens, V. Shatokhin, and A. Buchleitner, *Rep. Prog. Phys.* **67**, 45 (2004); A. Kenfack and K. P. Singh, *Phys. Rev. E* **82**, 046224 (2010).
- [18] L. Machura, M. Kostur, P. Talkner, J. Łuczka, and P. Hänggi, *Phys. Rev. Lett.* **98**, 040601 (2007).
- [19] D. Speer, R. Eichhorn, and P. Reimann, *Europhys. Lett.* **79**, 10005 (2007).
- [20] D. Speer, R. Eichhorn, and P. Reimann, *Phys. Rev. E* **76**, 051110 (2007).
- [21] M. Kostur, J. Łuczka, and P. Hänggi, *Phys. Rev. E* **80**, 051121 (2009).
- [22] M. Kostur, L. Machura, P. Talkner, P. Hänggi, and J. Łuczka, *Phys. Rev. B* **77**, 104509 (2008).
- [23] J. Nagel, D. Speer, T. Gaber, A. Sterck, R. Eichhorn, P. Reimann, K. Ilin, M. Siegel, D. Koelle, and R. Kleiner, *Phys. Rev. Lett.* **100**, 217001 (2008).
- [24] D. Hennig, *Phys. Rev. E* **79**, 041114 (2009).
- [25] P. S. Landa and P. V. E. McClintock, *J. Phys. A* **33**, L433 (2000).
- [26] V. N. Chizhevsky, E. Smeu, and G. Giacomelli, *Phys. Rev. Lett.* **91**, 220602 (2003).
- [27] L. Du and D. Mei, *Phys. Rev. E* **85**, 011148 (2012).
- [28] C. Mulhern, *Phys. Rev. E* **88**, 022906 (2013).
- [29] M. C. Fischer, K. W. Madison, Q. Niu, and M. G. Raizen, *Phys. Rev. A* **58**, R2648 (1998).
- [30] J. L. Mateos, *Phys. Rev. Lett.* **84**, 258 (2000).
- [31] A. Kenfack, S. M. Sweetnam, and A. K. Pattanayak, *Phys. Rev. E* **75**, 056215 (2007).
- [32] M. Barbi and M. Salerno, *Phys. Rev. E* **62**, 1988 (2000).